

Fabrication of flexible supercapacitor through light scribe method to achieve high performance energy storage device

M.Sc. Thesis

By
LALIT BHARTI



**DISCIPLINE OF PHYSICS
INDIAN INSTITUTE OF TECHNOLOGY INDORE
JUNE 2018**

Fabrication of flexible supercapacitor through light scribe method to achieve high performance energy storage device

A THESIS

*Submitted in partial fulfilment of the
requirements for the award of the degree
of*
Master of Science

by
LALIT BHARTI



DISCIPLINE OF PHYSICS
INDIAN INSTITUTE OF TECHNOLOGY INDORE
JUNE 2018



INDIAN INSTITUTE OF TECHNOLOGY INDORE

CANDIDATE'S DECLARATION

I hereby certify that the work which is being presented in the thesis entitled **Fabrication of flexible supercapacitor through light scribe method to achieve high performance energy storage device** in the partial fulfillment of the requirements for the award of the degree of **MASTER OF SCIENCE** and submitted in the **DISCIPLINE OF PHYSICS, Indian Institute of Technology Indore**, is an authentic record of my own work carried out during the time period from July 2016 to June 2018 under the supervision of Dr. Sudeshna Chattopadhyay, Associate professor, Discipline of physics, IIT Indore.

The matter presented in this thesis has not been submitted by me for the award of any other degree of this or any other institute.

**Signature of the student with date
(LALIT BHARTI)**

This is to certify that the above statement made by the candidate is correct to the best of my/our knowledge.

Signature of the Supervisor of

M.Sc. thesis

DR. SUDESHNA CHATTOPADHYAY

LALIT BHARTI has successfully given his/her M.Sc. Oral Examination held on **21 JUNE 2018**.

Signature(s) of Supervisor(s) of MSc thesis

Date:

Convener, DPGC

Date:

Signature of PSPC Member #1

Date:

Signature of PSPC Member #2

Date:

ACKNOWLEDGEMENTS

I take this opportunity to express my profound gratitude and deep regards to my respectful supervisor, ***Dr. Sudeshna Chattopadhyay*** for her exemplary guidance, monitoring and constant encouragement throughout the course of this project. I am grateful to my PSPC members ***Dr. Pankaj R. Sagdeo***, and ***Dr. Suman Mukhopadhyay*** for their valuable suggestions and guidance. I am also thankful to all faculty members of Physics Department for their guidance and motivation

I would like to acknowledge IIT Indore for providing basic infrastructure and extending all the necessary facilities. I would also like to acknowledge Sophisticated Instrument Centre (SIC), IIT Indore, for FESEM studies. I would like to acknowledge department of science and technology (DST), Government of India, New Delhi for providing us funds.

I am also thankful to my group members, Aakash Mathur, Ajaib Singh, Dipayan Pal, Rinki Singh and my classmates for their constant company throughout the project with the bottom of my heart.

LALIT BHARTI

Abstract

For Electrode materials in supercapacitors, surface area and porosity is a key feature to achieve high performance. Due to a high theoretical surface area ($>2600\text{m}^2/\text{g}$), promising flexibility, and high tensile strength, graphene and graphene based supercapacitors are getting the high region of interest from last few years. Reduced graphene oxide (RGO), material with 2D hexagonal structure of sp^2 carbons like graphene is preferably used at the place of graphene because of more readily available and possibilities of doping or other structural modifications to get better performance. By inspiring from these favourable properties, in this work, we have used RGO as an electrode material in supercapacitor system which was formed by reduction of graphene oxide by a simple and low-cost light scribe technique.

The chemical and structural characterization of material was carried out by XRD which shows the structural changes after reduction by lightscribe method. Optical images were taken with an optical microscope to observe the changes in colour contrast after reduction. SEM was also used to see the morphological change in material, and finally Raman spectroscopy was used to verify the RGO formation. Electrochemical characterization techniques cyclic voltammetry (CV), galvanostatic charge discharge (GCD) and electrochemical impedance spectroscopy (EIS) were used to study the capacitive performance of the double layer supercapacitor system with RGO as an electrode material. Samples with different light scribe cycles and different thicknesses were fabricated and characterized to study the effect of lightscribe cycles to achieve higher performance in terms of higher specific capacitance. Supercapacitor sample with higher numbers of scribing cycles at 14 cycles shows higher specific areal capacitance of $8.75\text{ mF}/\text{cm}^2$ compare to lower scribed sample at 7 scribe cycles which shows areal capacitance of $0.765\text{ mF}/\text{cm}^2$ at a same current density of $0.125\text{ mA}/\text{cm}^2$. As second step of the experiment, surface modification was done by ultrathin coating of ZnO on RGO by atomic layer deposition technique (ALD) technique, which is a surface controlled layer-by-layer deposition method. Effect of ZnO coating was also studied by comparing the capacitive performance of the light scribed RGO sample before and after coating, and few layers of ZnO coated sample shows the enhancement of the specific areal capacity. To further achieve highest possible capacitance by optimizing the number of scribe cycles during reduction and effects of ZnO coating on RGO. To achieve highest possible capacities of such low cost highly desirable flexible system, the optimization of laser scribing parameters (for the uncoated system) and ALD coating parameters (to control the thickness and structure of the thin coating) are in progress.

TABLE OF CONTENTS

	Content	Page no.
Chapter 1	Introduction	1
1.1	Introduction	1
Chapter 2	Experimental techniques	5
2.1	Material synthesis	5
2.2	Structural techniques	7
2.2.1	X-ray Diffraction (XRD)	7
2.2.2	Scanning Electron Microscopy	9
2.2.3	Raman spectroscopy	10
2.3	Electrochemical techniques	13
2.3.1	Cyclic voltammetry (CV)	13
2.3.2	Galvanostatic Charging Discharging (GCD)	15
2.3.3	Electrochemical Impedance spectroscopy (EIS)	16
Chapter 3	Results and Discussion	18
3.1	Structural properties	18
3.1.1	Optical microscope analysis	18
3.1.2	SEM/EDAX	18
3.1.3	Resistivity measurement	19
3.1.4	X-ray Diffraction (XRD)	21
3.1.5	Raman spectroscopy	22
3.2	Electrochemical properties	24
3.2.1	Cyclic Voltammetry (CV)	24
3.2.2	Galvanostatic Charge Discharge (GCD)	32
3.1.3	Electrochemical Impedance Spectroscopy (EIS)	37
Chapter 4	Conclusion and future scope	38
References	List of references	40

LIST OF FIGURES

Figure no.	content	Page no.
1.1	Schematic comparing power density and energy density of various devices	2
2.2	Schematic representation of charge storage mechanism	3
1.3	Illustration of the transformation of graphite to reduced graphene oxide	4
2.1	Schematic of steps for complete supercapacitor device preparation	5
2.2	Representation of Bragg's law	7
2.3	Powder XRD machine at SIC, IIT Indore	8
2.4	Schematic of Scanning electron microscope	9
2.5	Schematic representation of Raman transitions	10
2.6	Vibration modes of graphene	11
2.7	Schematic representation of different Raman processes	12
2.8	CV Excitation Signal	14
2.9	figure showing phase difference between current and potential	16
2.10	Nyquist plot for an EDLC with its equivalent circuit.	17
3.1	Optical microscope images for scribed patterns made by light scribe.	18
3.2	EDAX plot for (a) GO and (b) RGO	18
3.3	SEM images for GO and RGO	19
3.4	I-V curve for RGO (by four-probe method).	20
3.5	XRD pattern for GO, RGO and bare PET.	21
3.6	Raman spectra of GO and RGO	22
3.7	CV curve of pristine RGO sample (7 cycles)	24
3.8	CV curve of pristine RGO sample (14 cycles)	25
3.9	CV curve of sample_2 (6 cycle ZnO doped RGO)	25
3.10	Scan rate vs. areal capacity of pristine RGO.	29
3.11	Scan rate vs. areal capacity of ZnO coated RGO.	29
3.12	Scan rate vs. areal capacity of pristine RGO (14 cycles).	30
3.13	Scan rate vs. current plot for ZnO coated RGO sample.	31
3.14	GCD curve of pristine RGO sample (7 cycles) in potential window of 0 to 1 V	32
3.15	GCD curve of 14 scribe cycle pristine RGO sample in potential window of 0 to 1 V	33

3.16	GCD curve of ZnO coated RGO sample in potential window of 0 to 1 V	33
3.17	Stability curve of ZnO coated RGO sample up to 1000 charge-discharge cycles.	36
3.18	Nyquist plot for ZnO coated RGO and pristine RGO samples.	37

LIST OF TABLES

Table no.	Content	Page no.
3.1	C/O ratios for (a) GO and (b) RGO	19
3.2	Resistivity measurements of GO and RGO.	20
3.3	Areal capacity calculated at various scan rates from 1mV/s to 100 mV/s for pristine RGO (7 cycles).	26
3.4	Areal capacity calculated at various scan rates from 1mV/s to 100 mV/s for pristine RGO (14 cycles).	27
3.5	Areal capacity calculated at various scan rates from 1mV/s to 100 mV/s for ZnO coated RGO by ALD.	28
3.6	Specific capacitance calculated at different current rates from 0.125 mA/cm ² to 0.500 mA/cm ² within a potential window of 0 to 1 V for ZnO coated RGO sample.	34
3.7	Specific capacitance calculated at different current rates from 0.125 mA/cm ² to 0.500 mA/cm ² within a potential window of 0 to 1 V for pristine RGO sample (7 cycles)	34
3.8	Specific capacitance calculated at different current rates from 0.125 mA/cm ² to 0.500 mA/cm ² within a potential window of 0 to 1 V for pristine RGO sample (14 cycles)	35

Acronyms

GO	Graphene oxide
RGO	Reduced graphene oxide
EDLC	Electrochemical Double layer capacitance
ALD	Atomic layer deposition
CV	Cyclic voltammetry
WE	Working electrode
RE	Reference electrode
CE	Counter electrode
GCD	Galvanostatic Charging Discharging
EIS	Electrochemical impedance spectroscopy
GCD	Galvanostatic Charging Discharging
AC	Alternate current
DC	Direct current

Chapter 1

Introduction

Energy is the capacity of doing work. In physics, energy is a quantitative property that can be transferred to an object in order to perform some work on the object. Energy is a conservative quantity. According to the law of energy conservation, Energy cannot be created or destroyed, it can only be converted in one to another form. The law of energy conservation created the necessity of energy storage to store the energy when available by converting it into a suitable form and use it when needed.

There are two kinds of energy sources, renewable and non-renewable. Nonrenewable sources like fossil fuel, coal, oil, natural gas etc. sources which are limited on earth and cannot be renewed after ended once whereas renewable sources are the sources which are naturally available on a human timescale like solar and wind energy. All kind of energy from various sources can be converted into electrical energy to use by people. After conversion, this electrical energy is needed to be stored to use it when needed. Energy storage devices are used to store this energy.

Electric energy storage devices is a system used for storing electric energy when needed and provides it when required. Electric Energy storage devices. EES can be divided into below categories.

1. Battery
2. Capacitor
3. Supercapacitor or EC

Batteries store energy through a faradaic process which involves reduction or oxidation of some chemical substance at an electrode in presence of an electrolyte as a charge carrier medium. Whereas capacitors are devices where electric energy is stored directly in form of charge with a non-faradaic process, where only charges move without any redox reaction. Supercapacitor or electrochemical capacitor or Ultracapacitor is the device having same charge storage mechanism like conventional capacitors but it stores charge in an electric double layer that forms at the interface between an electrode and an electrolyte solution[4]. Batteries are the energy storage devices which store electric energy in form of chemical energy.

Due to the different charge storage mechanism, they exhibit different energy and power density outputs, reaction time, cyclability, stability and lifetime. In batteries faradaic current is generated by some redox reaction of electrode species at the interface, these oxidation and reduction processes changes the molecular structure of electrode material, due to these redox reactions

charging and discharging of batteries are slow and since this deformation of electrode in every charge-discharge cycle cyclability of batteries are limited to some thousands of cycles, Whereas supercapacitors have much higher life cyclability with non-faradaic type of mechanism, due to fast charge transfer process supercapacitors have fast charging and discharging time and high power density where batteries process high energy density and can provide current for much longer time compared to supercapacitors at lower power densities. All these parameters can be compared together in figure 1.1 below.

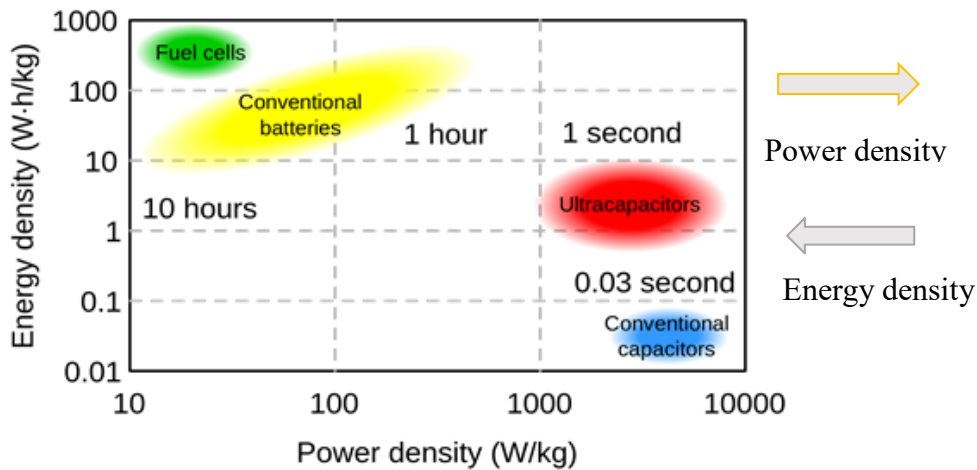


Fig. 1.1: Schematic comparing power density and energy density of various devices[2]

Depending on different performance parameters all these devices have their different region of usage in real life, like Li-ion batteries in mobile phones for high energy densities and supercapacitors in electric vehicles for high power densities.

Depending upon working mechanism, Supercapacitors are divided into three categories.

1. EDLC (Electrochemical Double layer capacitance)
2. Pseudo Capacitor
3. Hybrid Capacitor

Electrostatic Double-layer capacitance is a system where electrostatic storage of the electric energy is achieved by the separation of charges which creates two layers of charges called Helmholtz double layer, both layers act

like a single capacitance and total capacitance is the sum of capacitance by both layers. Surface area and pore size of electrode material and size of electrolyte ions play a big role for EDLC. Supercapacitors with carbon based electrodes come in EDLC category like Graphene and RGO electrode based supercapacitors.

In pseudocapacitance, electrochemical storage of the electric energy is achieved by some faradaic redox reactions at electrode interfaces, processing charge generation mechanism like batteries and due to this mechanism pseudo capacitance have relatively high capacitance and lower charge-discharge cyclability. Supercapacitor having metal oxide and conducting polymers as electrode material comes in this category. Whereas hybrid capacitors are the asymmetric type of supercapacitors where used electrodes are with differing characteristics, one exhibiting mostly electrostatic capacitance and the other mostly electrochemical capacitance.

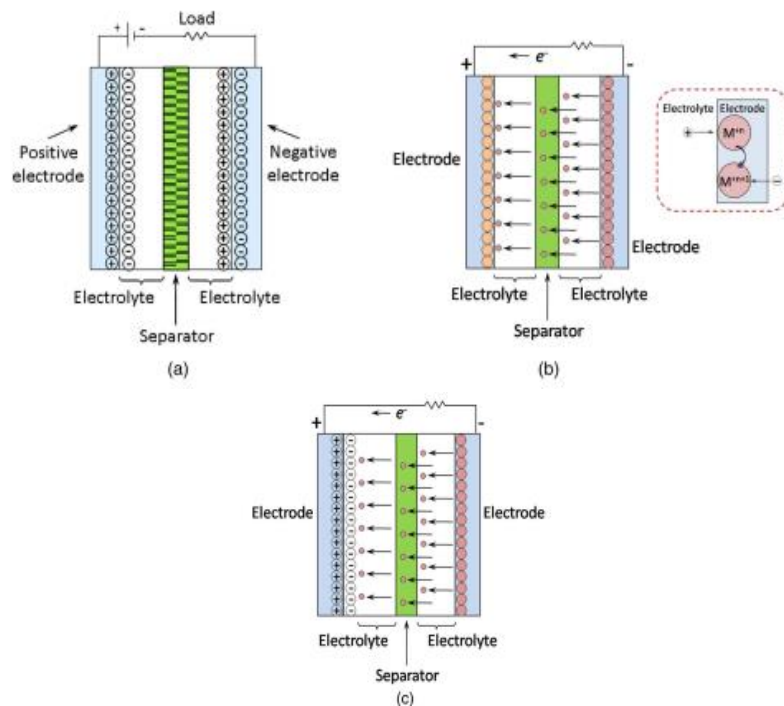


Fig. 1.2: Schematic representation of charge storage mechanism for (a) EDLC, (b) pseudocapacitance (c) hybrid capacitance [5]

For EDLC, graphene is a promising material by having a high theoretical surface area ($>2600\text{m}^2/\text{g}$), promising flexibility, and tensile strength of 130 GPa[6]. The objective of our study is to fabricate the graphene-based supercapacitors through light scribing method to achieve high performance by surface modification of material. Production of graphene derivatives such as graphene oxide (GO) is more convenient than graphene sheets[7]. RGO is obtained by reduction of oxygen atoms from graphene oxide (GO). GO can be chemically[8], thermally[9], or mechano-chemically[10] reduced to form graphene each of which has some advantages over others. Reduced graphene oxide (RGO), material with 2D hexagonal structure of sp^2 carbons like graphene is preferably used at the place of graphene because of more readily available and possibilities of doping or other structural modifications to get better performance, where graphene does not allow it because of its stable/inactive 2D hexagonal structure. The RGO will contain numerous defect sites, which are favourable for electrochemical applications[11].

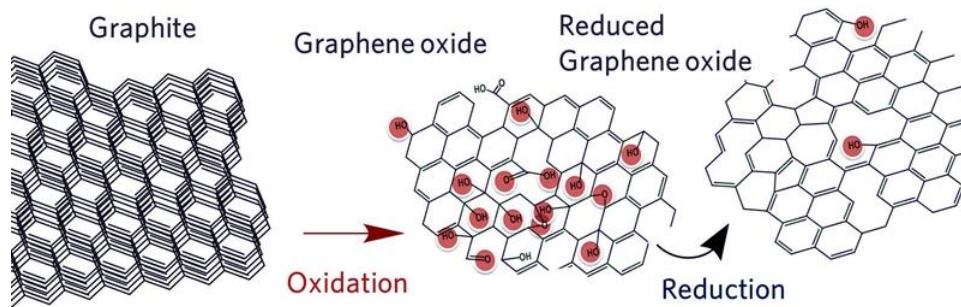


Fig. 1.3: Illustration of the transformation of graphite to reduced graphene oxide[3].

In our work light scribe method is used for reduction of Graphene Oxide, in which an IR light source is used to irradiate radiation (of wavelength $\sim 780\text{nm}$) to material surface to reduce it into RGO from GO.

Chapter 2

Experimental techniques

2.1 Material synthesis

2.1.1 GO solution preparation:

Graphene Oxide (GO) powder was purchased from Alfa aesar and Techinstro which was synthesized by Hummer's method which is a conventional method of GO powder preparation. 148 mg GO powder was weighted by and 40 mL deionized water was added to make 40 mL aqueous GO solution with a concentration of 3.7 mg/mL, while pH of the solution was maintained between 11-12 by 1M NaOH solution. This solution was ultra-sonicated for 1 hour to get a uniform GO suspension into water.

2.1.2 GO to RGO preparation

This GO solution was dropcasted on a PET of thickness 50 microns. About 16 mL solution was used to cover complete area of lightscribe disc, then the dropcasted film was dried for 24 hours under air ambient to make a uniform GO film on PET as substrate. Lightscribe disc was put into a commercially available lightscribe burner drive, which makes scribed patterns on the coated disc. Number of cycles can be controlled while scribing. Samples with different number of cycles were made.

2.1.2 ZnO coating by ALD:

To study the effect of ZnO coating, ZnO coated samples were made by Atomic layer depositor, in which ZnO molecules are deposited layer-by-layers by reaction of two precursors in an isolated chamber. Di-methyl Zinc was used as the first precursor followed by H₂O as the second precursor and by reaction of both precursors with the substrate, ZnO was formed on the sample surface. Number of ALD cycles were kept to be 6 which forms 6 atom layers on the substrate surface and light scribing was done after ZnO coating.

2.1.3 Electrolyte preparation:

1g PVA powder was added in 10 mL of 1M H₂SO₄ solution and mixed at 80c temperature by a magnetic stirrer until mixture becomes transparent.

2.1.3 Supercapacitor device fabrication

The scribed electrode patterns were cut out and Cu tape was applied to make proper terminal connections and exposed area of Cu tape was insulated by kapton tape. Polymer-based PVA+ H₂SO₄ gel electrolyte was coated over the device and dried for 24 hours under air ambient, after drying, whole device was covered by kapton tapes to avoid further drying of electrolyte and avoid any external damages.

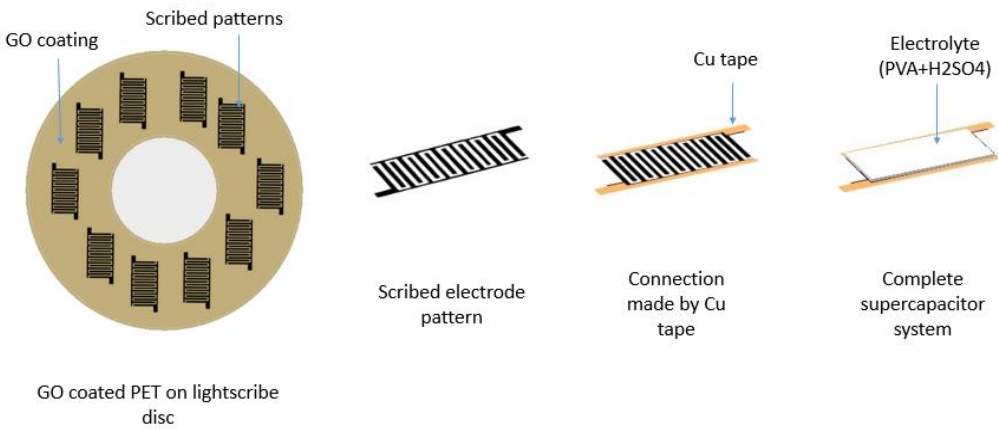


Fig. 2.1: Schematic of steps for complete supercapacitor device preparation

2.2 Structural techniques

2.2.1 X-ray Diffraction (XRD)

2.2.1.1 Principle

XRD is a rapid analytic technique used for phase detection of crystalline material and provides information about crystal structures like crystal planes present in the crystalline material. XRD technique also provides information for stress in the crystal structure, crystallinity, chemical structure, particle size etc.

X-rays are electromagnetic waves having a wavelength of 0.1 Å to 100 Å and energy in the range of 120 eV to 120 keV. XRD is based on scattering of incident X-rays by specimen material. When X-rays are incident on a specimen the crystalline solid acts as a diffraction grating and gives a diffraction pattern after the constructive interference of monochromatic X-rays by following the Bragg's law given as

$$n\lambda = 2d \sin \theta$$

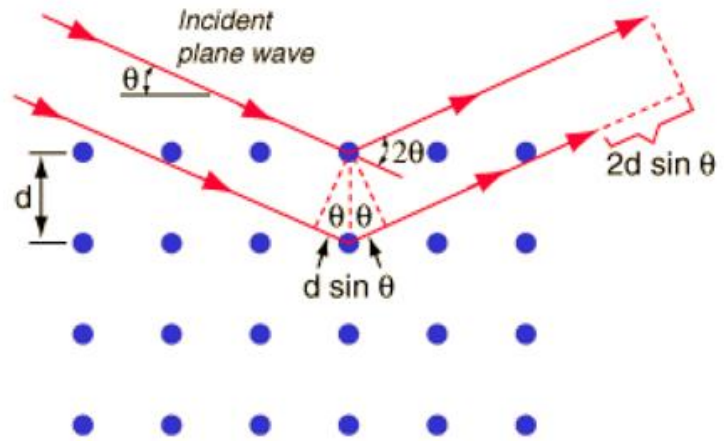


Fig. 2.2: Representation of Bragg's law[1].

Where n is the order of diffraction, λ is the wavelength of incident X-rays, d is the interlayer spacing between the planes and θ is the angle between incident X-ray beam and lattice plane in the crystal[1].

Diffracted X-rays are detected by an X-ray detector and intensities of X-rays are counted with respect to diffracted angle 2θ within a given 2θ range.

All possible diffraction angles of the lattice are recorded due to random orientation of material. The intensity peaks at different 2θ angles gives information about planes present in crystalline structure and present crystalline material can be identified by analyzing available XRD data and comparing references.

2.2.1.2 Instrumentation

1. X-ray tube: It is the filament which generates X-rays
2. Sample holder
3. Detector: Detects the X-rays and counts the intensity.

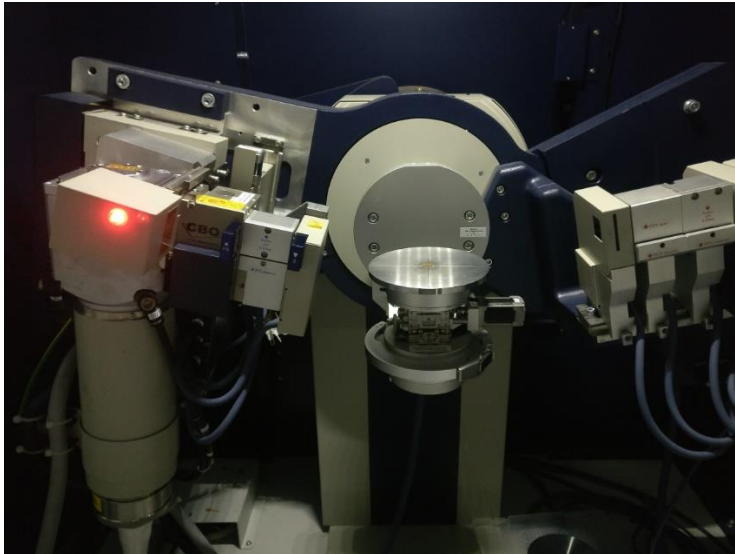


Fig. 2.3: Powder XRD machine at SIC, IIT Indore

2.2.2 Scanning Electron Microscopy:

Scanning electron microscopy is a useful technique which gives information about topography, surface structure, morphology and composition of the sample, provides images with high resolutions up to 1nm. SEM is an electron microscope that produces images of a sample by scanning the surface with a focused high energy beam of electrons.

In SEM high energy electron beam is incident on the sample surface and these high energy electrons interact with the electron of the samples material. Incident electrons may be absorbed, conducted or reflected at the sample surface, absorbed electrons interact with electrons of the sample and this interaction produces secondary electrons. Some electrons get backscattered from the sample. These secondary electrons are detected by detectors and give useful information about material structure like surface morphology. Backscattered electrons give information about chemical composition of the material. In SEM electron beam of high energy is used which have a shorter wavelength, since the wavelength of any electromagnetic wave is inversely proportional to resolution, SEM has much higher resolution than any optical microscope.

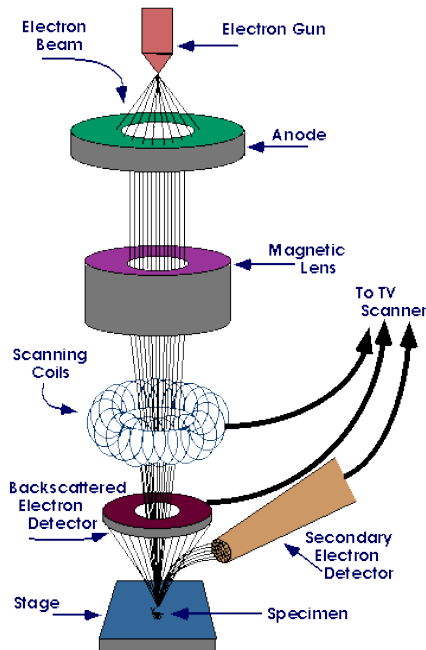


Fig. 2.4: Schematic of Scanning electron microscope[12].

Principal and working mechanism:

An electron beam of high energy is generated from the electron gun, accelerated by the anode and passes through magnetic lenses. Electron beam is focused by these magnetic lenses and incident on a specific area of the sample where electrons interact with the sample and produce secondary and backscattered electrons which were then detected by different detectors. This gives information about sample structure morphology and composition. For SEM sample must be a conductive sample to avoid accumulation of charges by absorbed electrons and reflection of other electrons. For nonconductive sample gold coating is need to be done, it also preserves sample during scanning process under high energy electron beam. Thus ejected electrons provide information about surface structure, morphology, size, shape and texture of surface and X-rays, emitted from the depth of the sample surface, provide element composition information.

2.2.3 Raman spectroscopy:

Raman spectroscopy is the spectroscopic technique based on inelastic scattering of monochromatic light by a sample. During this process, monochromatic light is scattered and this scattering of light changes the frequency of light. It makes difference between incident and scattered light. When photons are incident on a sample some energy they interact with sample molecules and some energy is transferred to sample molecules, this energy transfer makes frequency change between incidents and scattered light. This change in frequency gives information about frequency transition in sample molecules by rotation, vibration and other Raman active modes in the molecule.

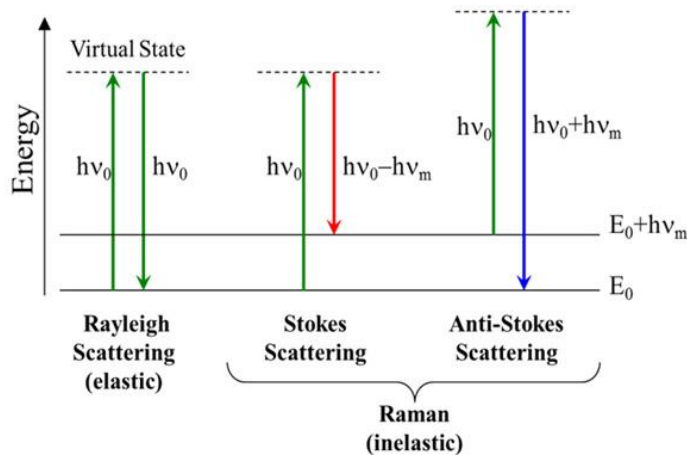


Fig. 2.5: Schematic representation of Raman transitions[13].

Three kinds of interactions are possible depending upon the type of energy transition:

1. Rayleigh scattering: When a molecule with no Raman active modes absorbs a light of some frequency ν_0 , molecule goes in a transition and reach a virtual state and comes back to the same vibrational state with emitting light of the same frequency ν_0 , this is called Rayleigh scattering.
2. When a molecule with some Raman active modes absorbs photons of some frequency ν_0 , at the time of interaction some energy is transferred to Raman active modes and the emitted frequency of scattered light is reduced by ν_m , and frequency of scattered light becomes $\nu_0 - \nu_m$, this is called Stokes frequency.
3. When a Raman active molecule is already in excited vibration state at the time of interaction, after absorbing light of some frequency ν_0 , excited molecule comes back to basic vibrational level with emitting light having a frequency $\nu_0 + \nu_m$, this frequency is called anti-stokes frequency.

A Raman spectrometer consists (a) a light source, which illuminates the sample with UV, visible or near IR light, (b) wavelength selector or filter, which selects a monochromatic light and (c) a detector by which scattered light is detected. Raman spectra is a plot between the frequency of light and scattered light intensity. By analyzing the spectrum, Raman spectrum provides information about active modes and bonds present in the molecule.[14]

Raman spectra of graphene:

Vibration modes associated with the G and the 2D peak of graphene are shown in figure 2.6, Both vibration modes give corresponding peaks in Raman spectra.

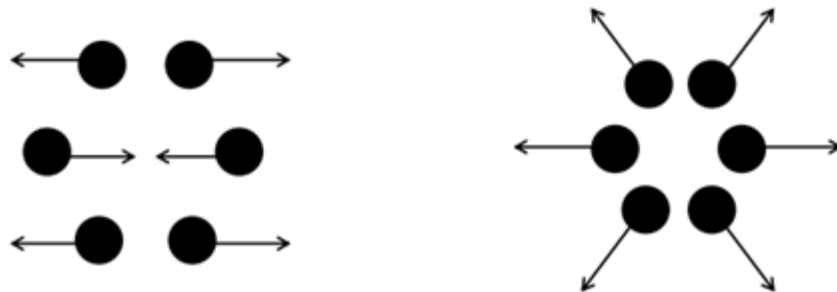


Fig. 2.6: Vibration modes of graphene[15].

Raman processes involved in the activation of the G, 2D peaks and D, D' defect peaks:

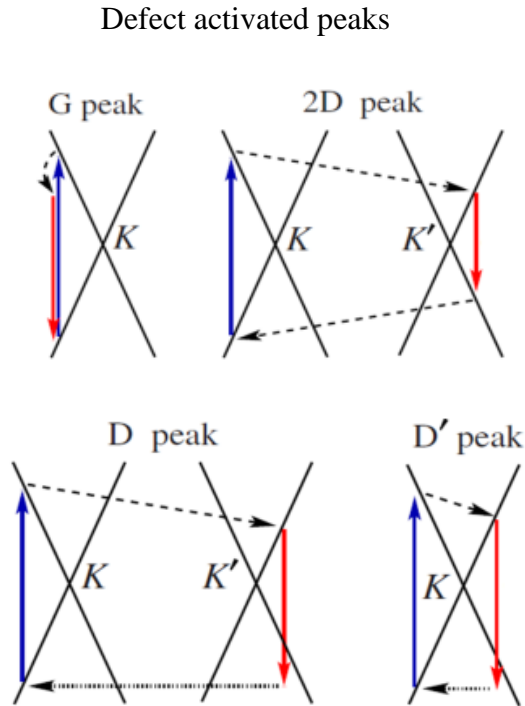


Fig 2.7: Schematic representation of different Raman processes[15].

The blue (up) arrows correspond to the absorption of a photon and the creation of an electron/hole pair. The red (down) arrows represent the radiative recombination of the electron/hole pair. The dashed arrows depict the inelastic charge scattering from phonons or the elastic scattering from defects.

For graphene, 2D peak of spectra is affected by the defects present and for graphene oxide which is containing many defect sides, 2D peak is not present in Raman spectra. Raman spectra of graphene oxide have G and D two bright peaks, which give information about bonds present.

2.3 Electrochemical techniques

2.3.1 Cyclic voltammetry (CV)

Cyclic voltammetry (CV) is a powerful and popular electro-chemical technique commonly employed to investigate the electrochemistry of molecular species during an electrochemical process like oxidation and reduction of some species[16]. In CV, a voltage signal is applied on the system with a fixed scan rate and current response of the system is measured during the process, this plot between potential and current is called voltammogram or cyclic voltammogram.

Electrode Setup for CV: For electrochemical characterizations, three types of electrodes are used in the setup.

1. Working electrode (WE)
2. Reference electrode (RE)
3. Counter electrode (CE)

Working electrode:

In an Electrochemical system, working electrode is the electrode on which the reaction of interest is Occurring. Common working electrodes are made of inert materials such as Au, Ag, Pt etc. For characterization of electrode material in an electrochemical process, the material of the working electrode is the material under investigation. The size and shape of the working electrode vary according to their usage and applications.

Reference electrode:

The reference electrode is the electrode which is used as a point of reference in the electrochemical system for an electrochemical process, it has a stable and well-known electrode potential which is taken as a reference potential for the potential control and measurement. The high stability of the reference electrode potential is usually reached by employing a redox system with constant (buffered or saturated) concentrations of each participant of the redox reaction. The current flow through the reference electrode is always kept to be approximately zero (ideally, zero) which is achieved by using the CE to close the current circuit in the electrochemical cell together by putting a very high input impedance with the electrometer (>100 G-Ohm)[16, 17].

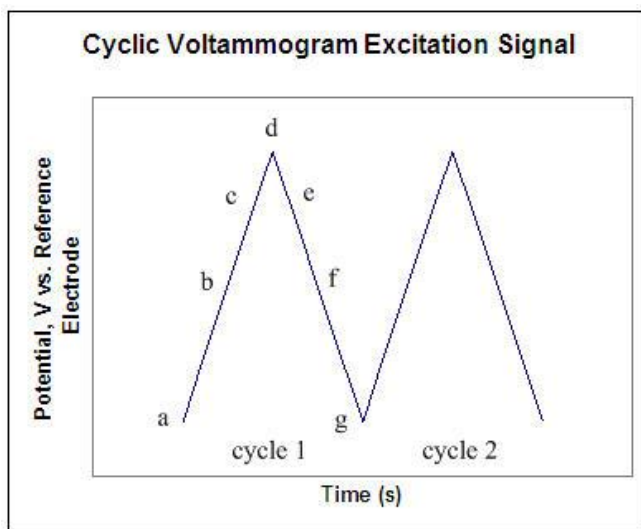
Counter electrode:

The counter electrode (or auxiliary electrode), is an electrode which is used to close the current circuit in the electrochemical cell. It is also made of an inert material and usually it does not participate in the electrochemical

reaction. It keeps the current flow through RE zero by flowing all current through itself. Since the current is flowing between the WE and the CE, the total surface area of the CE must be always higher than the area of the WE so that it will not be a limiting factor in current flow and in the kinetics of the electrochemical process for the system under investigation.

In three electrode system, the potential is always measured between the WE and the RE and the current is always measured between the WE and CE. Whereas, in two electrode system RE and CE are shorted altogether on one electrode opposite of WE. Here the potential across the complete cell is measured. This includes contributions from the CE/electrolyte interface and also from the electrolyte itself. The two-electrode configuration can be used where the behaviour of the whole cell is under investigation and precise control of the interfacial potential across the WE electrochemical interface is not critical. This setup is typically used with energy storage or conversion devices like batteries, supercapacitors, fuel cells, photovoltaic panels etc.

In Cyclic Voltammetry, The potential of the working electrode is measured against a reference electrode which maintains a constant potential, and the resulting applied potential produces an excitation signal such as shown in figure 2.8[18]. In the forward scan, the potential first scans negatively, starting from a greater potential (a) and ending at a lower potential (d). The potential extrema (d) is called the switching potential, from this point, the potential starts to scan positively. At this point, the voltage is sufficient enough to cause an oxidation or reduction of an analyte. The reverse scan from (d) to (g) is the region where the potential scans positively. Figure 2.8 shows a typical reduction occurring from (a) to (d) and an oxidation occurring from (d) to (g). In EDLC mechanism reduction and oxidation of analyte represent the charging and discharging of the system respectively.



.Fig. 2.8: CV Excitation Signal[18].

The current response is recorded by the system and plotted together against the applied potential signal at a fixed scan rate. Voltammogram for EDLC is nearly rectangular without any oxidation or reduction peaks since generation of double layer is directly depends on potential applied without any redox reaction in the system. Specific capacitance of system can be calculated by voltammogram. Since capacitance is charge divided by potential and charge is current multiplied by time,

The Specific areal capacitance is given by the formula[6]

$$C = \frac{1}{a \cdot v \Delta V} \int I dV$$

Where $\int I dV$ is the mathematical area of voltammogram, v is scan rate, ΔV is a potential window and a is the area of the active material. This relation also shows that the value of capacitance decreases with increasing scan rates.

2.3.2 Galvanostatic Charging Discharging (GCD):

In this techniques a fixed value of current is passed through the system until the system reached to a fixed potential point, depends on the chosen potential window, time taken during charging and discharging is calculated and specific capacitance is measured by the formula given below[6],

$$C = \frac{I \cdot \Delta t}{m \Delta V}$$

and specific areal capacitance is given by[6],

$$C = \frac{I \cdot \Delta t}{a \cdot \Delta V}$$

Where I is the applied current, Δt is the discharge time, m is the mass of active material, a is the area of active material and ΔV is the voltage window. EDLC shows higher specific capacitance for lower current rates due to the slow kinetics of electrochemical system, which gives more opportunities to electrolyte ions to accumulate on electrode material efficiently.

2.3.3 Electrochemical Impedance Spectroscopy (EIS)

Electrochemical impedance spectroscopy (EIS) is a powerful technique for characterizing a wide variety of electrochemical systems and for determining the contribution of electrolytic processes in these systems.

In a DC system where only DC (direct current) is flowing through a sample, the current through the sample is directly proportional with the potential developed across the sample, and resistance of system can be calculated by Ohm's law which is shown below,

$$R = V/I$$

Where V is the developed voltage and I is the current through the system. Above formula is sufficient for calculating resistivity of DC systems, but when AC current and AC components like capacitor, inductor etc. are involved in the system, then the behaviour of the system becomes more complex. A more generalized parameter, Impedance is measured here instead of resistivity which involves resistance and other frequency dependent parameters like capacitance, inductance etc. depending on the elements present in the system. In EIS a potential signal is applied to the system and current response is measured with a phase difference at different frequencies within a wide frequency range.

In DC elements like a resistor, current and voltage are in the same phase but in a capacitor which is a frequency dependent system, current leads voltage by 90° of phase difference.

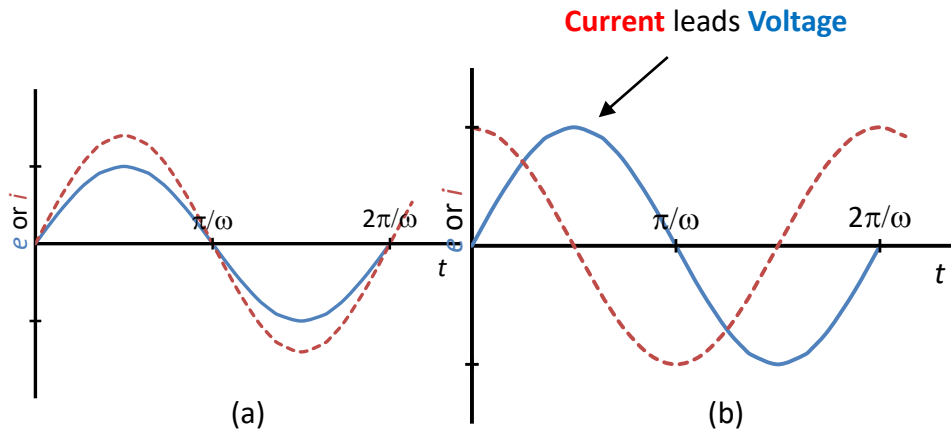


Fig. 2.9: Figure showing phase difference between current and potential. for (a) resistor with no phase difference and (b) capacitor where current leads voltage by 90° .

The provided excitation signal, expressed as a function of time, has the form of

$$V(t) = V_o \sin (\omega t)$$

Where $V(t)$ is the potential at time t , V_o is the amplitude of the excitation signal and ω is the [4, 5] radial frequency, and $\omega = 2\pi f$

Whereas, the current which is the response signal is shifted in phase by ϕ is given by,

$$I(t) = I_o \sin (\omega t + \phi)$$

Now from Ohm's law expression for impedance is given by

$$\begin{aligned} Z(t) &= V(t)/I(t) \\ &= V_o \sin \omega t / I_o \sin (\omega t + \phi) \\ &= Z_o \sin \omega t / \sin (\omega t + \phi) \end{aligned}$$

Thus impedance is presented by magnitude Z_o with some phase. Impedance can be written as,

$$\begin{aligned} Z &= Z_o \exp (i\phi) \\ &= Z_o (\cos\phi + i \sin\phi) \end{aligned}$$

This complex expression contains a real and an imaginary part, the real part of impedance is plotted against the imaginary part, this plot is called Nyquist Plot. The impedance can be represented as a vector of length $|Z|$ on the Nyquist Plot. And the angle between this vector and the X-axis is frequency (f).

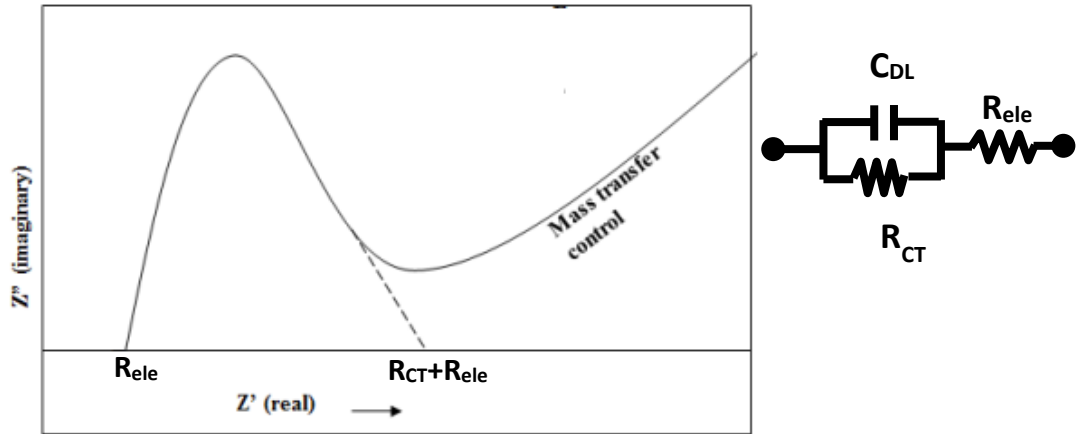


Fig. 13: Nyquist plot for an EDLC with its equivalent circuit.

Where C_{DL} is the double layer capacitance, R_{ele} is the Electron Transfer Resistance and R_{CT} is Uncompensated (electrolyte) Resistance.

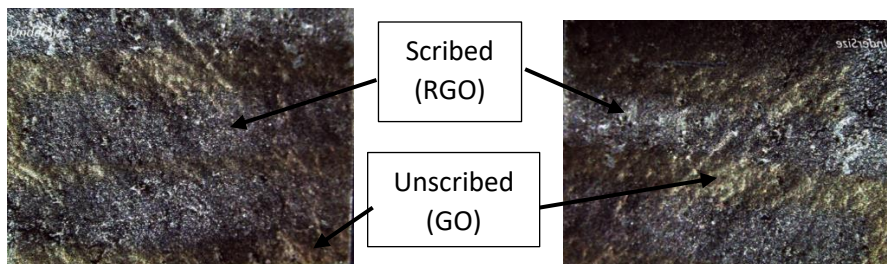
Chapter 3

Results and Discussion

3.1 Structural properties

3.1.1 Optical microscope analysis

Optical microscope images:



Resolution 15X

Fig. 3.1: Optical microscope images for scribed patterns made by light scribe.

Optical images have been taken of scribed patterns by an optical microscope with 15x resolution. After scribing RGO and GO patterns can be easily identified in an optical microscope image due to the big contrast in optical transparency between the RGO and GO areas, the reduced graphene oxide regions became much darker than the GO region[19].

3.1.2 SEM/EDAX

SEM(Scanning electron microscopy) has been done to analyze morphological changes in graphene oxide material during reduction. EDX measurement has been taken for compositional analysis of samples which shows higher C to O ratio after light scribing and indicates the reduction of oxygen containing functional groups from graphene oxide during light scribe.

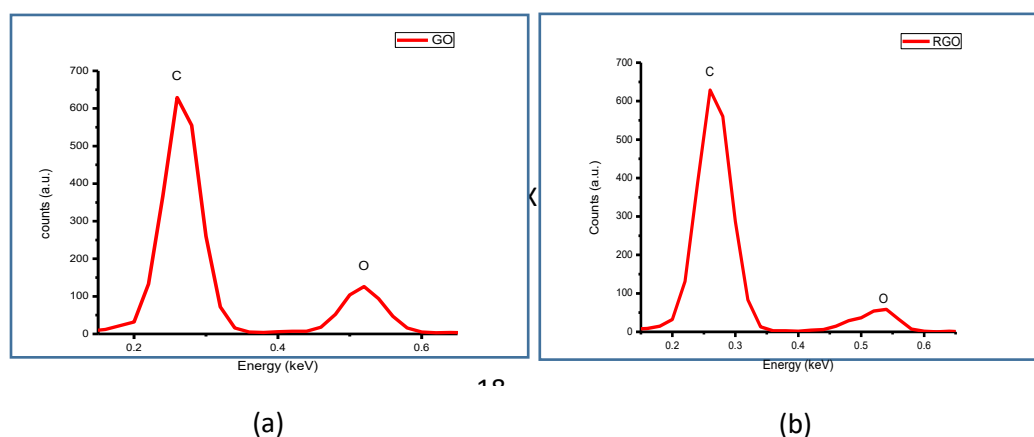


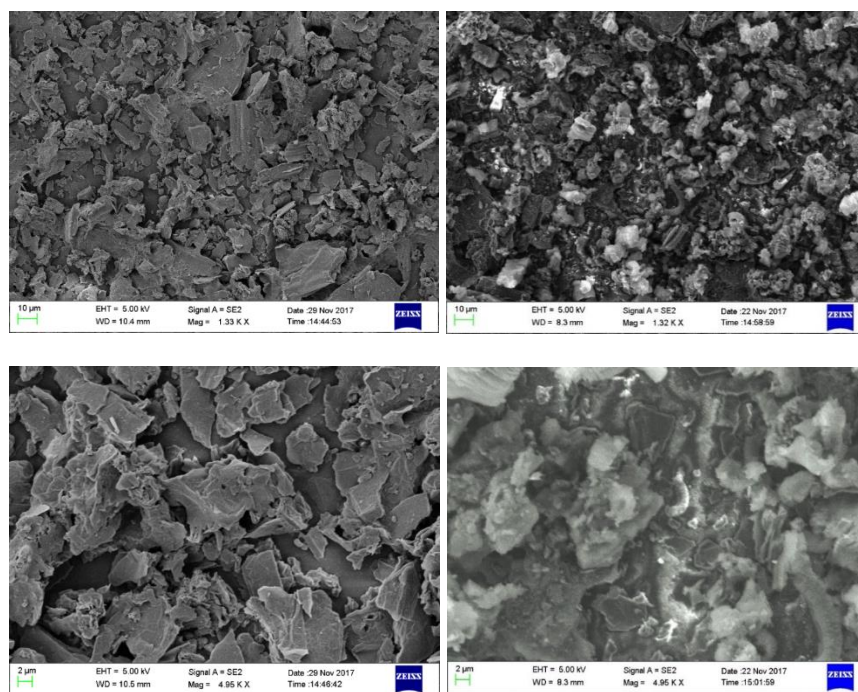
Fig. 3.2: EDAX plot for (a) GO and (b)

Element (GO)	Weight%	Atomic%	Element (RGO)	Weight%	Atomic%
C K	65.97	72.08	C	77.65	82.23
O K	34.03	27.92	O	22.35	17.77
Totals	100.00		Totals	100.00	
O/C ratio		0.37	O/C ratio		0.21

(a)

(b)

Table 3.1: C/O ratios for (a) GO and (b) RGO



GO (before light scribe)

RGO (after light scribe)

Fig. 3.3: SEM images for GO and RGO

3.1.3 Resistivity measurement by four probe method

The resistivity of material film on PET substrate has been measured by four probe method before and after light scribing. Increments in conductivity have been observed by resistivity measurement before and after ~10 cycles of light scribing on GO film, indicates the formation of Reduced GO (RGO) by eliminating oxygen and hydroxyl groups which make GO sheets electrically insulating by interrupting moving electrons that conduct current through GO sheets.

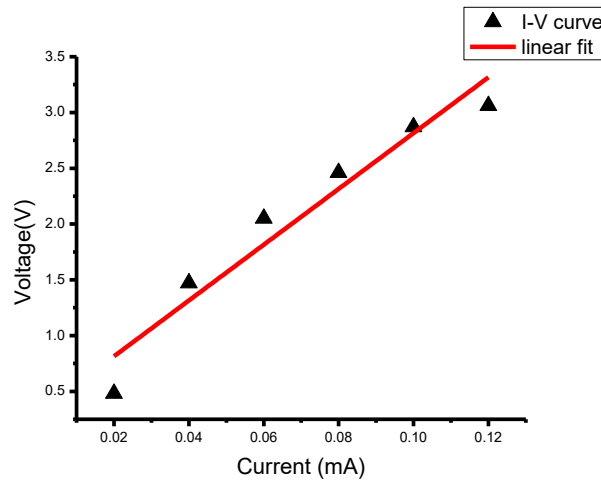


Fig. 3.4: I-V curve for RGO (by four-probe method).

	Resistivity
Before light scribe (GO)	>100 M Ω .cm
After light scribe (RGO)	6 k Ω .cm

Table 3.2: Resistivity measurements of GO and RGO.

3.1.4 XRD

Characterization techniques like XRD and Raman spectroscopy have been used to verify the reduction process and formation of reduced graphene oxide from graphene oxide. X-ray diffraction patterns have been observed for structural analysis of GO and RGO material on PET film as substrate. The XRD patterns shown in figure 3.5 shows a peak at $2\theta = 11.4^\circ$ which is the corresponding peak of GO[20]. GO has relatively larger interlayer distance due to the formation of carboxyl and hydroxyl functional groups, which is $\sim 0.79\text{nm}$. This peak is absent after light scribing due to the removal of these oxygen-containing functional groups. This suggests the reestablishment of conjugated graphene network with sp^2 carbons[20] and shows change in the structure of material after scribing. Intense peaks at $2\theta = 25.9^\circ$ and $2\theta = 44.5^\circ$ are characteristic peaks of PET which is used as substrate for all samples[21]. The changes of structure during reduction from GO to RGO is further confirmed by Raman spectrum analysis of samples before and after scribing.

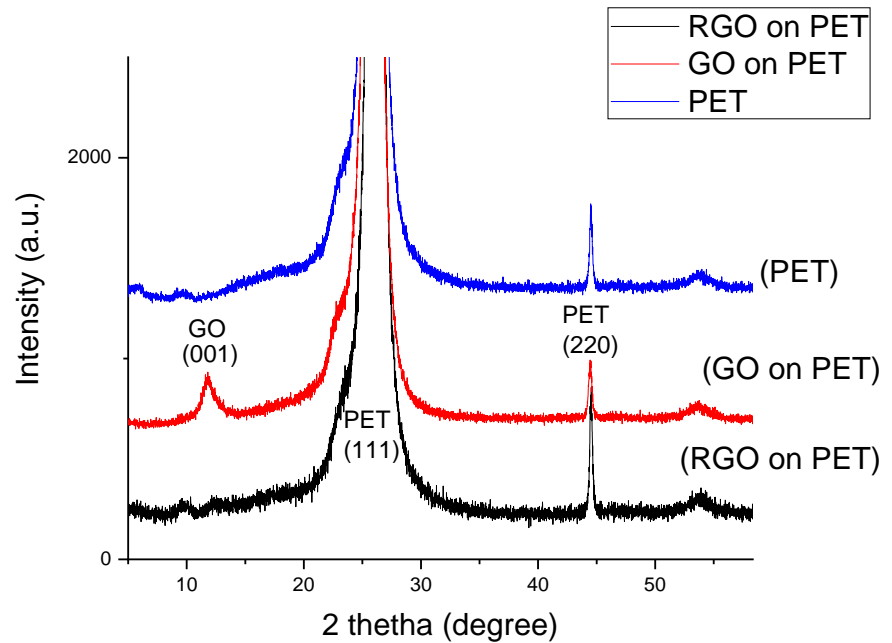


Fig. 3.5: XRD pattern for GO, RGO and bare PET.

3.1.5 Raman spectroscopy

In figure 3.6, Raman spectra of GO and RGO on PET substrate is shown, where D band refers to the sp^2 carbon structure and G band refers to the disorders present in structure due to oxygen-containing functional groups. Change in D band to G band intensity ratio I_D/I_G exhibits decrease of defects in structure after reduction[22].

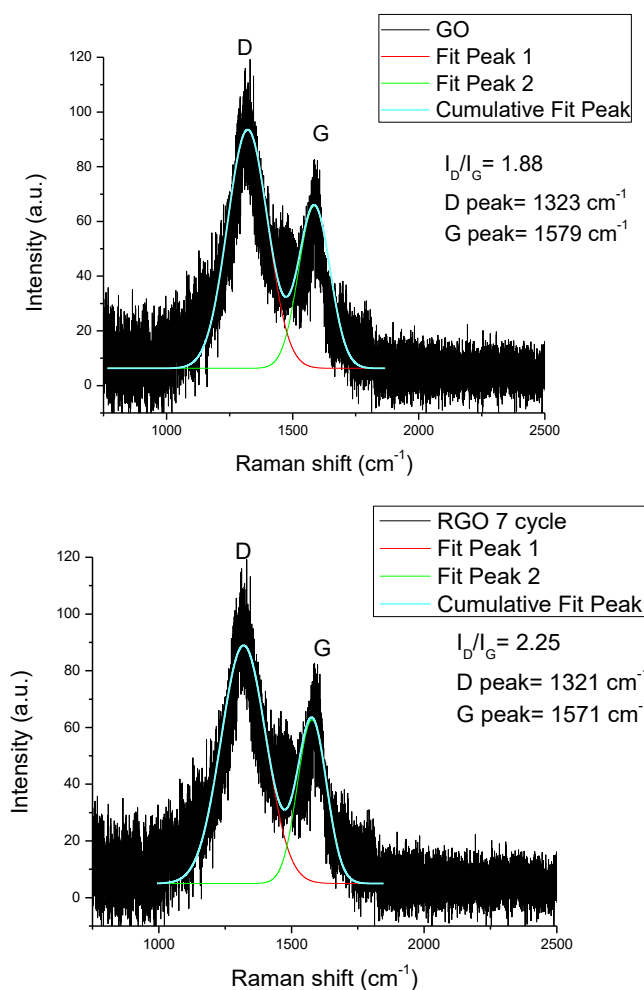


Fig. 3.6: Raman spectra of GO and RGO

The Raman spectra for GO and RGO are shown in above figure. The spectrum of GO in figure 3.6 shows D band peak at 1323 cm^{-1} due to the defects and G band peak at 1579 cm^{-1} for the inplane vibrations. After reduction, D band peak shows a very small change and G band peak is down shifted from 1579 cm^{-1} to 1571 cm^{-1} (fig. 18) owing to the self healing characteristics of the RGO that recovers the hexagonal network of carbon atoms with defects[22]. This confirms the successful reduction of GO to RGO. Intensity ratio I_D/I_G is found to be 1.88 for GO and 2.25 for RGO,

this slightly increased value of I_D/I_G also favours the reduction of GO in RGO during the light scribe process[22].

In summary, observations from the optical microscope and SEM images show the morphological changes in graphene oxide before and after reduction. XRD technique and Raman spectroscopy have been used for structural analysis of material samples. Results from XRD and Raman spectroscopy confirms the proper reduction of graphene oxide to reduced graphene oxide.

3.2 Electrochemical properties

3.2.1 Cyclic Voltammetry (CV)

Cyclic voltammetry analysis of both samples has been done in a potential window of 0 to 1V at various scan rates with a two-electrode system and PVA-H₂SO₄ as a gel-based electrolyte. Specific capacitance of system was calculated at all scan rates. The specific areal capacitance of the system is given by[6]

$$C = \frac{1}{av \Delta V} \int IdV$$

Where v is the scan rate in mV/s, ΔV is the potential window of analysis and a is the area of active material in cm².

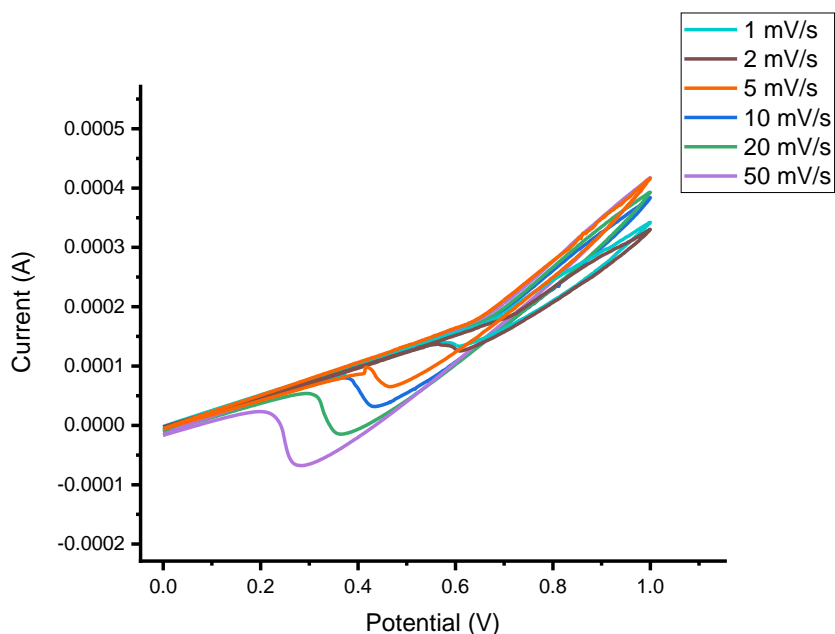


Fig. 3.7: CV curve of pristine RGO sample (7 cycles) at scan rate of 1mV/s, 2mV/s, 4 mV/s, 5 mV/s, 7.5 mV/s, 10 mV/s, 20 mV/s and 50 mV/s in potential window of 0 to1 V.

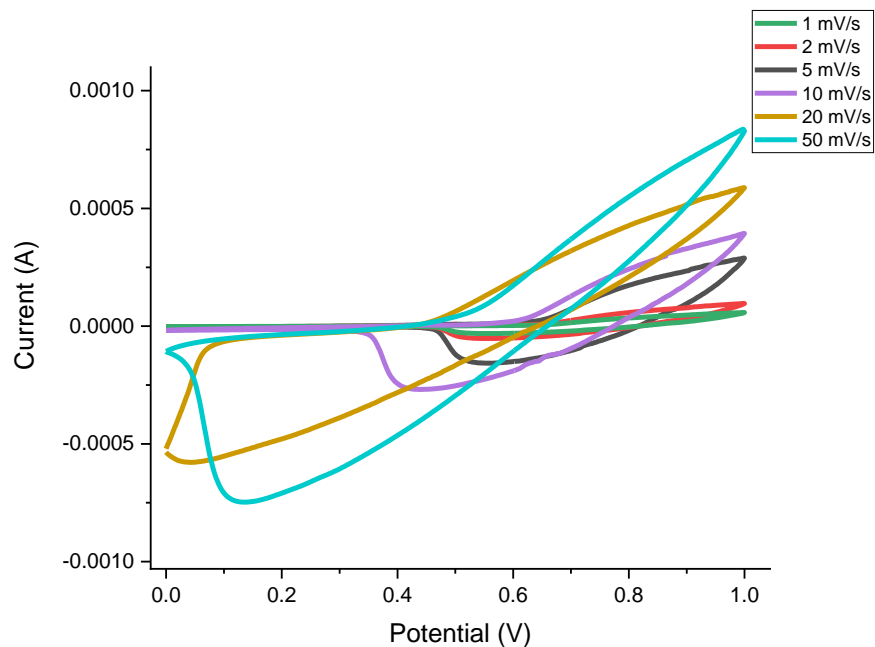


Fig. 3.8: CV curve of pristine RGO sample (14 cycles) at scan rate of 1mV/s, 2mV/s, 4 mV/s, 5 mV/s, 7.5 mV/s, 10 mV/s, 20 mV/s and 50 mV/s in potential window of 0 to1 V.

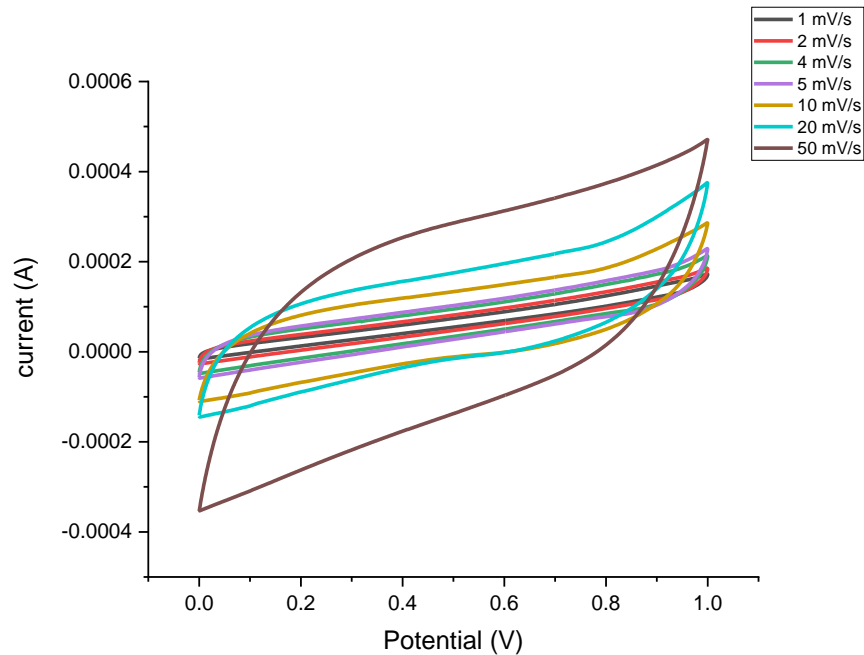


Fig. 3.9: CV curve of sample_2 (6 cycle ZnO doped RGO) at scan rate of 1mV/s, 2mV/s, 3mV/s, 4 mV/s, 5 mV/s, 7.5 mV/s, 10 mV/s, 20 mV/s in the potential window of 0 to 1V.

CV curve of pristine RGO (7 cycles), pristine RGO (14 cycles) and ZnO doped RGO sample is shown in figure 3.7, 3.8 and 3.9 respectively. All three CV curves were compared to study the working mechanism of charge storage, a reduction peak was observed in CV curve of pristine RGO and CV curve was not rectangular in shape which shows pseudocapacitance type of behaviour due to presence of unreduced GO[23], where CV curve of ZnO doped RGO was observed perfectly rectangular in shape which shows EDLC type of charge storage mechanism of system. This indicates proper reduction and EDLC type of working mechanism after ZnO coating on RGO by ALD. By increasing the number of cycles in pristine RGO sample, specific capacitance of the system was increased which show better reduction of graphene oxide compares to low cycles. Specific areal capacitance of both samples was calculated and mentioned in the table below. For the supercapacitor system capacitance of the system decreases with increasing scan rates. As the scan rates increases in CV process interaction between electrode and electrolyte becomes inefficient due to high charge transfer rates, the diffusion of electrolyte ions into electrode structure becomes difficult due to fast charge transfer process and therefore the capacitance of system decreases with higher scan rates.

Scan rate (mV/s)	Voltage window (V)	Mathematical area (mA.V)	Specific Capacitance (mF/cm²)
1	1	0.014	7.11
2	1	0.010	2.60
4	1	0.020	2.52
5	1	0.022	2.28
10	1	0.027	1.37
20	1	0.038	0.97
50	1	0.052	0.52
75	1	0.031	0.21
100	1	0.051	0.26

Table 3.3: Areal capacity calculated at various scan rates from 1mV/s to 100 mV/s for pristine RGO (7 cycles).

Scan rate (mV/s)	Voltage window (V)	Mathematical area (mA.V)	Specific Capacitance (mA/cm²)
1	1	0.022	11.0
2	1	0.037	9.43
5	1	0.081	8.11
10	1	0.129	6.47
20	1	0.276	6.90
50	1	0.372	3.72
100	1	0.314	1.57
200	1	0.270	0.67

Table 3.4: Areal capacity calculated at various scan rates from 1mV/s to 100 mV/s for pristine RGO (14 cycles).

Scan rate (mV/s)	Voltage window (V)	Mathematical area (mA.V)	Specific Capacitance (mF/cm ²)
1	1	0.020	10.0
2	1	0.034	8.58
4	1	0.060	7.56
5	1	0.073	7.37
10	1	0.133	6.68
50	1	0.349	3.49
100	1	0.461	2.30

Table 3.5: Areal capacity calculated at various scan rates from 1mV/s to 100 mV/s for ZnO coated RGO by ALD.

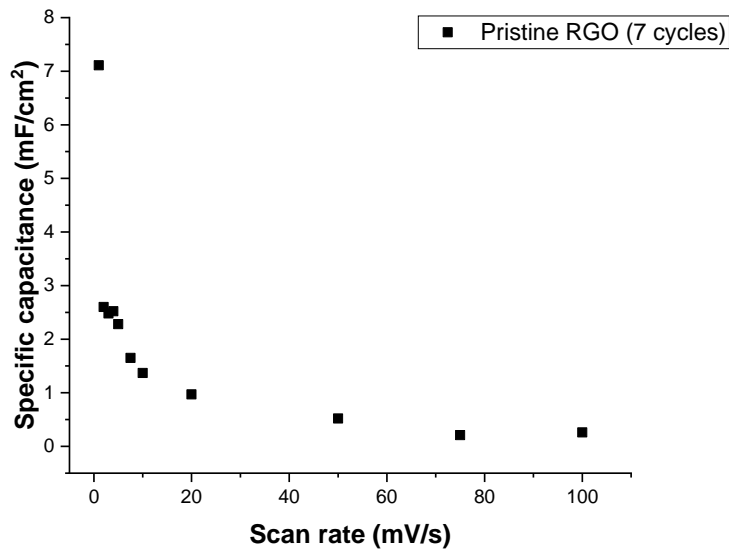


Fig. 3.10: Scan rate vs. areal capacity of pristine RGO.

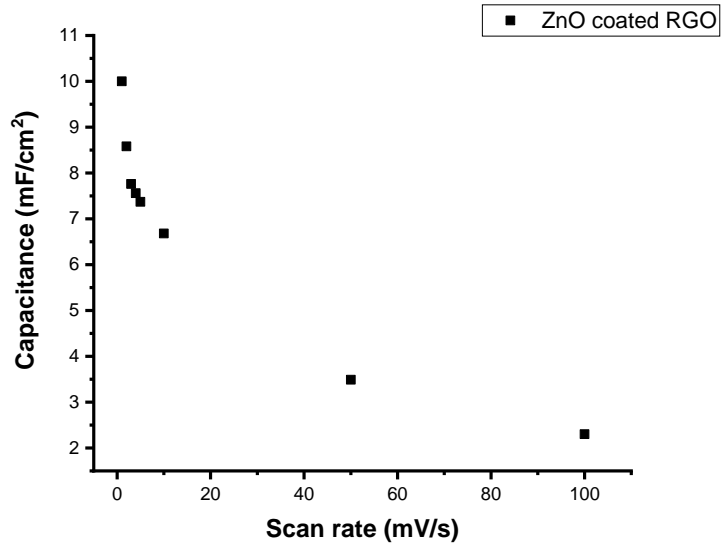


Fig. 3.11: Scan rate vs. areal capacity of ZnO coated RGO.

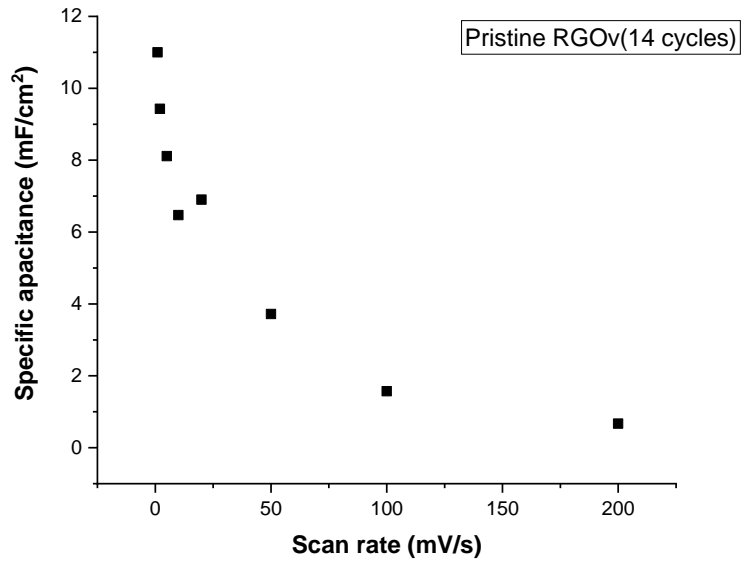


Fig. 3.12: Scan rate vs. areal capacity of pristine RGO (14 cycles).

By calculated specific areal capacitance in table 3.3, 3.4 and 3.5, a comparative study of specific capacitance of all devices was done successfully. Sample with higher scribe numbers (14 cycles) shows higher capacitance sample with ZnO coated shows higher specific areal capacitance compare to pristine RGO sample (7 cycles). Pristine RGO (7 cycles) device shows areal capacitance of 7.11 mF/cm² at scan rate of 1 mV/s where ZnO coated RGO shows areal capacitance of 10 mF/cm² and

pristine RGO (14 cycles) shows areal capacitance of 11 mF/cm² at the same scan rate of 1 mV/s. Also, the study of scan rate vs. specific capacitance was done for all samples. In scan rate vs. specific capacitance curve, specific capacitance of ZnO coated RGO and pristine RGO (14 cycles) were decreasing gradually and more appropriately than pristine RGO sample (7 cycles) which was decreasing drastically after 1 mV/s point in curve, this indicates better diffusion of electrolyte ions on electrode surface in ZnO coated RGO sample and shows its better behaviour over pristine sample, also favours higher scribe cycles to achieve higher capacitance.

A study of plot between scan rate and current values at a fixed potential was done to check the charge storage mechanism type of made supercapacitor system. For EDLC type of charge storage mechanism relation between current and scan rate is given as[24]

$$I(v) = k_1 v$$

Where v is the scan rate and I is the current values at a fixed potential (v).

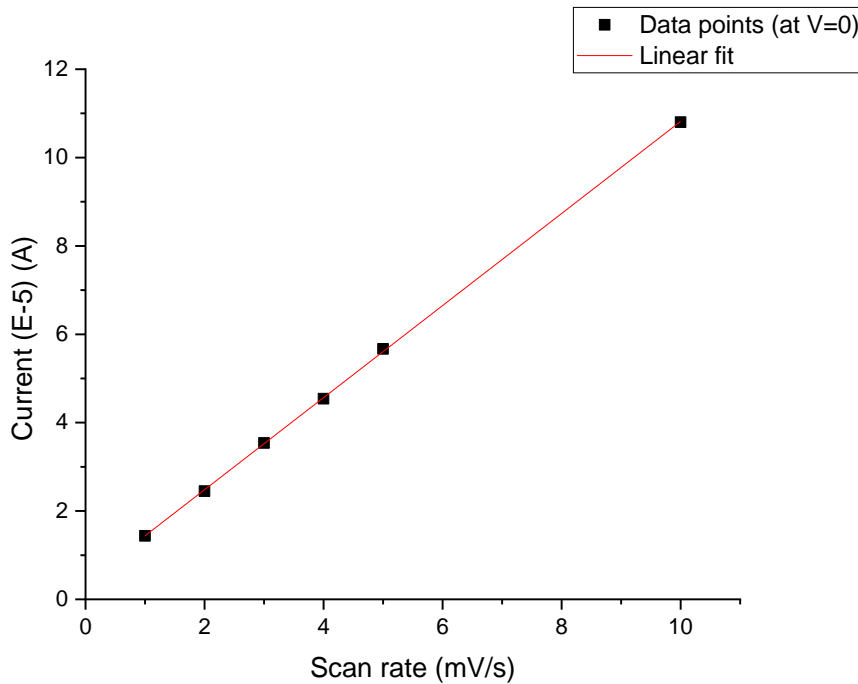


Fig. 3.13: Scan rate vs. current plot for ZnO coated RGO sample.

By this equation, for different current values in CV curve, current varies linearly with scan rate. For current vs. scan rate curve in figure 3.13 current shows a linear relationship with scan rates which indicates EDLC type of charge storage mechanism for our made supercapacitor system with ZnO coated RGO as an electrode material.

3.2.2 Galvanostatic Charge Discharge (GCD)

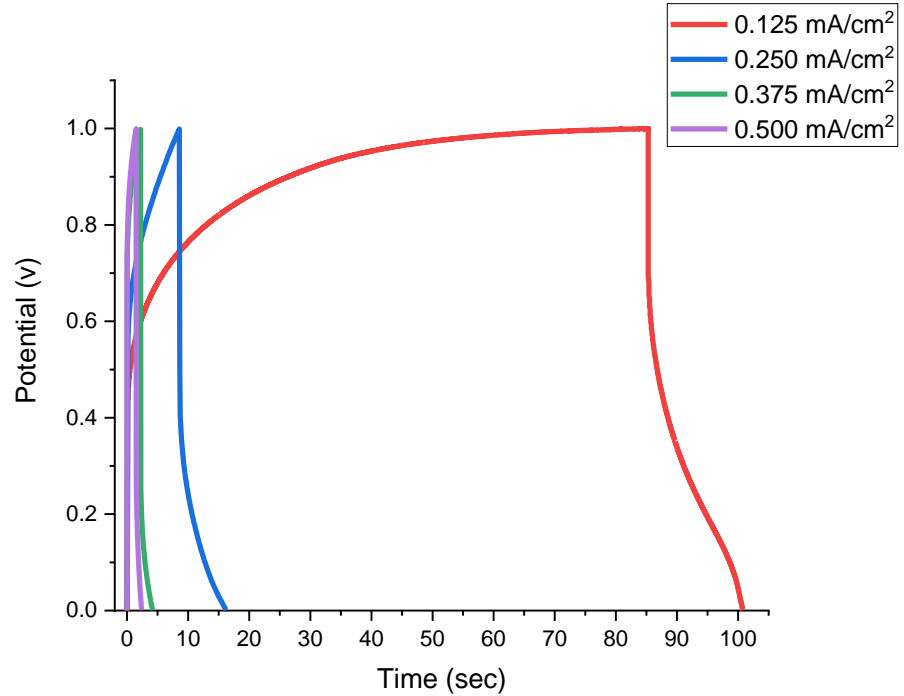


Fig. 3.14: GCD curve of pristine RGO sample (7 cycles) in potential window of 0 to 1 V at current densities of 0.125 mA/cm², 0.250 mA/cm², 0.375 mA/cm² and 0.500 mA/cm².

Galvanostatic charge discharge technique was used to study the capacitance behaviour at different current rates and specific capacitance was calculated at different current rates for both devices within a fixed potential window. In fig.26 GCD curve for pristine RGO sample is shown, GCD curves at current densities of 0.125 mA/cm², 0.250 mA/cm², 0.375 mA/cm² and 0.500 mA/cm² is shown in potential window of 0 to 1 V. In this current region, pristine RGO sample shows highest specific capacitance of 0.765 mF/cm² with discharge time of 15.3 seconds at current rate of 0.125 mA/cm². Specific capacitance values of pristine RGO sample at different current densities are calculated in below table which shows decrease in specific capacitance with increasing current rate values. At lower current rates charges get more time and opportunities to accumulate on electrode surface efficiently due to slow kinetics of system, this gives higher specific capacitance at lower current rates.

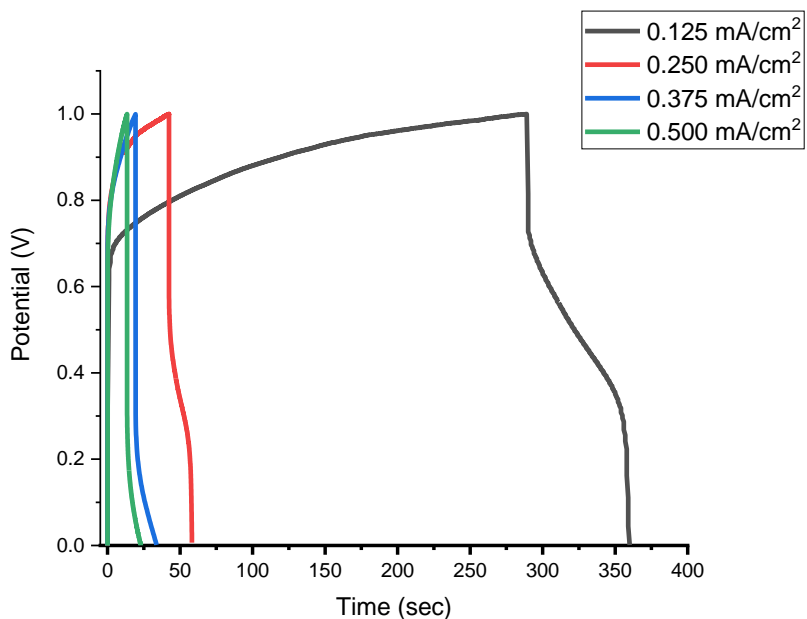


Fig. 3.15: GCD curve of 14 scribe cycle pristine RGO sample in potential window of 0 to 1 V at current densities of 0.125 mA/cm², 0.250 mA/cm², 0.375 mA/cm² and 0.500 mA/cm².

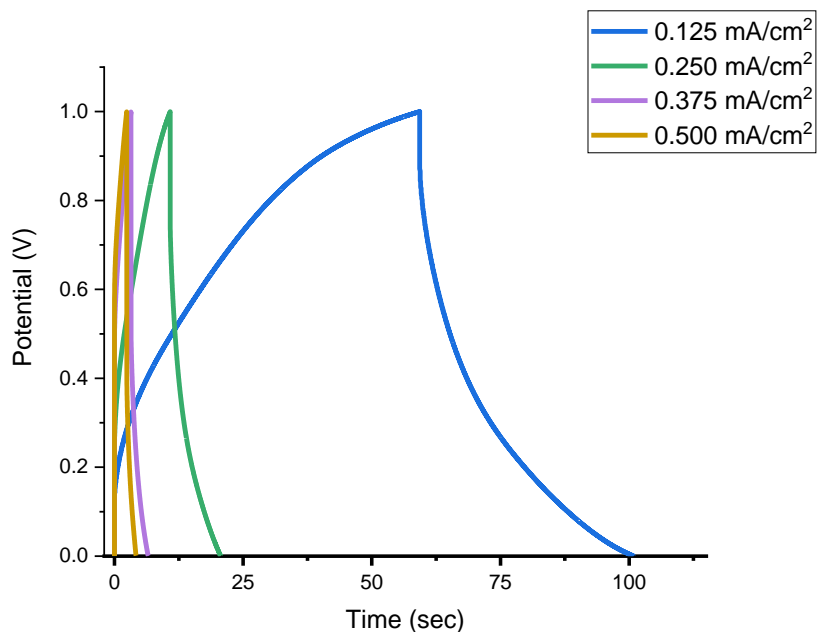


Fig. 3.16: GCD curve of ZnO coated RGO sample in potential window of 0 to 1 V at current densities of 0.125 mA/cm², 0.250 mA/cm², 0.375 mA/cm² and 0.500 mA/cm².

Sr. no.	Current rate (mA/cm ²)	Discharge time (sec)	Specific Capacitance (mF/cm ²)
1	0.125	15.3	0.765
2	0.250	7.68	0.576
3	0.375	1.98	0.19
4	0.500	0.9	0.11

Table 3.6: Specific capacitance calculated at different current rates from 0.125 mA/cm² to 0.500 mA/cm² within a potential window of 0 to 1 V for ZnO coated RGO sample.

Sr. no.	Current rate (mA/cm ²)	Discharge time (sec)	Specific Capacitance (mF/cm ²)
1	0.125	41.6	5.20
2	0.250	9.8	2.45
3	0.375	3.3	1.25
4	0.500	1.8	0.9

Table 3.7: Specific capacitance calculated at different current rates from 0.125 mA/cm² to 0.500 mA/cm² within a potential window of 0 to 1 V for pristine RGO sample (7 cycles)

Sr. no.	Current rate (mA/cm ²)	Discharge time (sec)	Specific Capacitance (mF/cm ²)
1	0.125	71	8.75
2	0.250	16.2	4.05
3	0.375	14.2	5.32
4	0.500	9.6	3.95

Table 3.8: Specific capacitance calculated at different current rates from 0.125 mA/cm² to 0.500 mA/cm² within a potential window of 0 to 1 V for pristine RGO sample (14 cycles)

Study of all three samples was also done by GCD technique. GCD plot for pristine RGO sample (14 cycles) and ZnO coated RGO sample is shown in figure 3.15 and figure 3.16 respectively and calculated specific capacitance is shown in table 3.7 and table 3.8 respectively at various current rates. Sample with 14 scribe shows higher capacitance of 8.75 mF/cm² compares to sample with 7 scribes which show specific capacitance of 0.765 mF/cm² at current rate of 0.125 mA/cm², this indicates better reduction of graphene oxide with higher numbers of light scribing. By increasing scribe cycles sample with 14 scribe cycles shows specific capacitance of 8.75mF/cm² at a same current rate of 0.125 mA/cm², this indicated better reduction of GO with higher number of scribes.

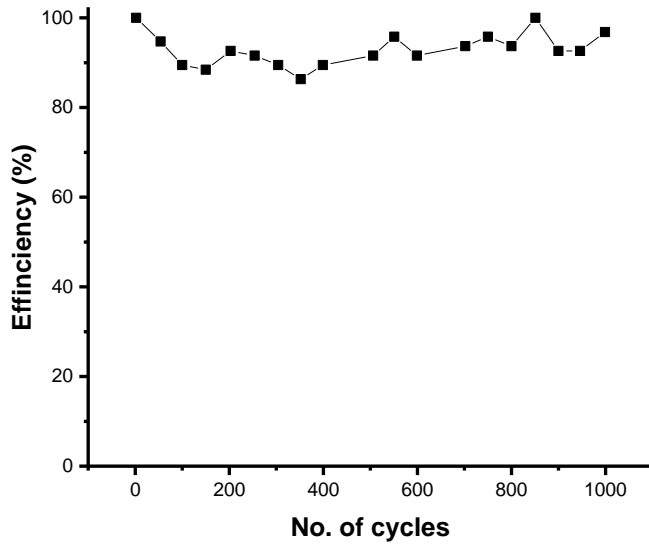


Fig. 3.17: Stability curve of ZnO coated RGO sample up to 1000 charge discharge cycles.

Stability curve is shown in fig. 30 of ZnO coated sample for 1000 charge discharge cycles which shows the specific capacitance is maintained more than 90% of its highest value for 1000 charge discharge cycles.

3.2.3 Electrochemical Impedance Spectroscopy (EIS)

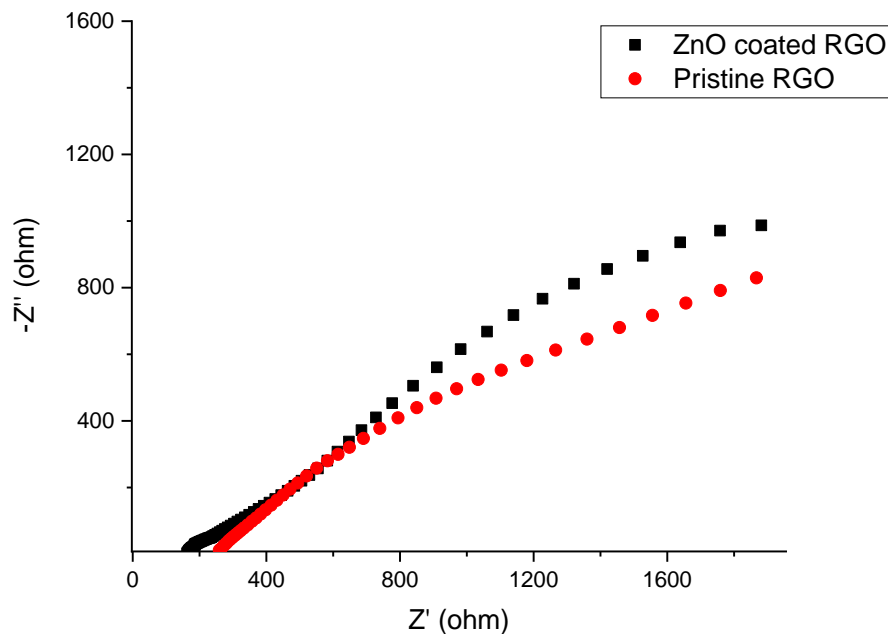


Fig. 3.18: Nyquist plot for ZnO coated RGO and pristine RGO samples.

Electrochemical impedance spectroscopy (EIS) was done to compare the capacitive performance of pristine RGO sample and ZnO coated RGO sample. EIS measurements were taken for both samples in the frequency range of 0.1 Hz to 100 kHz range at AC potential amplitude of 5 mV. EIS measurement data is shown in figure 3.18. In EIS plot above, in low-frequency region curve for ZnO coated RGO sample has a higher slope than pristine RGO sample which shows faster increment in imaginary part of impedance ($-Z''$) with respect to real part of impedance (Z') due to more effective formation of double layer on electrode surface in ZnO coated sample and thus shows higher specific capacitance compare to pristine RGO sample.

Chapter 4

Conclusion

Electrochemical double layer type of supercapacitor device was fabricated successfully with reduced graphene oxide as an electrode material. For Structural characterization SEM, XRD and Raman techniques and for electrochemical characterization by CV, GCD and EIS were done. ZnO coated RGO samples were made by atomic layer deposition method and performance was compared with pristine RGO samples by various electrochemical techniques.

After supercapacitor fabrication, work was done in two directions, performance with increasing number of lightscribe cycles and surface modification by ZnO coating on RGO surface by ALD technique both have studied. By increasing number of scribe cycles, the specific capacitance of system is increasing with scribe cycles. For pristine RGO with 14 scribe cycles, CV and GCD curves were compared with pristine 7 cycles sample where sample with 14 cycles shows higher capacitance of 8.75 mF/cm^2 at current rate of 0.125 mA/cm^2 in GCD. ZnO coated RGO sample also shows better performance in terms of higher specific capacitance than pristine RGO samples with same scribe cycles. For a given pristine light scribed RGO sample with low capacity (0.765 mF/cm^2) shows much higher capacity after ZnO (ultrathin) coating, which is 5.20 mF/cm^2 . It shows better performance of the device as an effect of ultrathin ZnO coating.

Future work and scope

Present work shows the behaviour of RGO based supercapacitor system with increasing and optimizing the laser scribe numbers and thickness of the GO/RGO films and gives a direction to get higher capacitance performance. Also, this work shows enhancement of specific capacitance by coating sample with ZnO by ALD technique with 6 cycles of coating.

For higher scribe cycles sample (14 cycles) with higher capacitance have been achieved, for which ZnO coating has to be done in future to attain higher capacitance and better performance.

By this study proper optimization of scribe rates to get highest possible specific capacitance is needed to be done in future. Further study of effects of ALD coating on RGO with different parameters, e.g. number of cycles, operation temperature etc., has to be done to optimize the growth parameters of the pristine and ZnO coated RGO samples, to achieve the best possible performance with high specific capacity of the system.

References

1. Bragg's law .
<http://hyperphysics.phy-astr.gsu.edu/hbase/quantum/bragg.html>
2. Storage Wars: Batteries vs. Supercapacitors
<http://berc.berkeley.edu/storage-wars-batteries-vs-supercapacitors/>.
3. Dahlberg T (2016) The first order Raman spectrum of isotope labelled nitrogen-doped reduced graphene oxide
4. Miller JR, Burke AF (2008) Electrochemical capacitors: challenges and opportunities for real-world applications. *The Electrochemical Society Interface* 17: 53
5. Vangari M, Pryor T, Jiang L (2013) Supercapacitors: Review of Materials and Fabrication Methods. *Journal of Energy Engineering* 139: 72-79. DOI doi:10.1061/(ASCE)EY.1943-7897.0000102
6. Amiri MH, Namdar N, Mashayekhi A, Ghasemi F, Sanaee Z, Mohajerzadeh S (2016) Flexible micro supercapacitors based on laser-scribed graphene/ZnO nanocomposite. *Journal of Nanoparticle Research* 18: 237. DOI 10.1007/s11051-016-3552-5
7. Dreyer DR, Park S, Bielawski CW, Ruoff RS (2010) The chemistry of graphene oxide. *Chemical Society Reviews* 39: 228-240. DOI 10.1039/B917103G
8. Alwarappan S, Liu C, Kumar A, Li C-Z (2010) Enzyme-Doped Graphene Nanosheets for Enhanced Glucose Biosensing. *The Journal of Physical Chemistry C* 114: 12920-12924. DOI 10.1021/jp103273z
9. Kang X, Wang J, Wu H, Aksay IA, Liu J, Lin Y (2009) Glucose Oxidase-graphene-chitosan modified electrode for direct electrochemistry and glucose sensing. *Biosensors and Bioelectronics* 25: 901-905. DOI <https://doi.org/10.1016/j.bios.2009.09.004>
10. Krishnamoorthy K, Kim SJ (2015) Mechanochemical preparation of graphene nanosheets and their supercapacitor applications. *Journal of Industrial and Engineering Chemistry* 32: 39-43. DOI <https://doi.org/10.1016/j.jiec.2015.09.012>
11. Ratinac KR, Yang W, Gooding JJ, Thordarson P, Braet F (2011) Graphene and Related Materials in Electrochemical Sensing. *Electroanalysis* 23: 803-826. DOI 10.1002/elan.201000545
12. Scanning Electrons Microscope
<http://ideal.vistalist.co/scanning-electrons-microscope/>.
13. Theory of Raman Scattering <http://www.bwtek.com/raman-theory-of-raman-scattering/>.
14. Wiberley NCLDS (1990) Introduction to Infrared and Raman Spectroscopy 3rd Edition

15. Eckmann A (2013) Raman spectroscopy of graphene, its derivatives and graphene-based heterostructures.
16. Elgrishi N, Rountree KJ, McCarthy BD, Rountree ES, Eisenhart TT, Dempsey JL (2018) A Practical Beginner's Guide to Cyclic Voltammetry. *Journal of Chemical Education* 95: 197-206. DOI 10.1021/acs.jchemed.7b00361
17. Metrohm electrochemistry <https://www.metrohm.com/en-gb/products-overview/electrochemistry>.
18. Kissinger PT, Heineman WR (1983) Cyclic voltammetry. *Journal of Chemical Education* 60: 702. DOI 10.1021/ed060p702
19. Xue Y, Zhu L, Chen H, Qu J, Dai L (2015) Multiscale patterning of graphene oxide and reduced graphene oxide for flexible supercapacitors. *Carbon* 92: 305-310. DOI <https://doi.org/10.1016/j.carbon.2015.04.046>
20. Moon IK, Lee J, Ruoff RS, Lee H (2010) Reduced graphene oxide by chemical graphitization. *Nature communications* 1: 73
21. Das S, Saha S, Sen D, Ghorai UK, Chattopadhyay KK (2014) Tailored defect-induced sharp excitonic emission from microcrystalline CuI and its ab initio validation. *Journal of Materials Chemistry C* 2: 6592-6600. DOI 10.1039/C4TC00955J
22. Zheng Q, Zhang B, Lin X, Shen X, Yousefi N, Huang Z-D, Li Z, Kim J-K (2012) Highly transparent and conducting ultralarge graphene oxide/single-walled carbon nanotube hybrid films produced by Langmuir–Blodgett assembly. *Journal of Materials Chemistry* 22: 25072-25082
23. Liu M, Zhang R, Chen W (2014) Graphene-Supported Nanoelectrocatalysts for Fuel Cells: Synthesis, Properties, and Applications. *Chemical Reviews* 114: 5117-5160. DOI 10.1021/cr400523y
24. Wang Y, Song Y, Xia Y (2016) Electrochemical capacitors: mechanism, materials, systems, characterization and applications. *Chemical Society Reviews* 45: 5925-5950. DOI 10.1039/C5CS00580A